Mapping weathering and alteration minerals in the Comstock and Geiger Grade areas using visible to thermal infrared airborne remote sensing data

R. Greg Vaughan* and Wendy M. Calvin
University of Nevada Reno, Department of Geological Sciences, Mail Stop 172, Reno, NV 89557

ABSTRACT

To support research into both precious metal exploration and environmental site characterization a combination of high spatial/spectral resolution airborne visible, near infrared, short wave infrared (VNIR/SWIR) and thermal infrared (TIR) image data were acquired to remotely map hydrothermal alteration minerals around the Geiger Grade and Comstock alteration regions, and map the mineral by-products of weathered mine dumps in Virginia City. Remote sensing data from the Airborne Visible Infrared Imaging Spectrometer (AVIRIS), SpecTIR Corporation's airborne hyperspectral imager (HyperSpecTIR), the MODIS-ASTER airborne simulator (MASTER), and the Spatially Enhanced Broadband Array Spectrograph System (SEBASS) were acquired and processed into mineral maps based on the unique spectral signatures of image pixels. VNIR/SWIR and TIR field spectrometer data were collected for both calibration and validation of the remote data sets, and field sampling, laboratory spectral analyses and XRD analyses were made to corroborate the surface mineralogy identified by spectroscopy.

The resulting mineral maps show the spatial distribution of several important alteration minerals around each study area including alunite, quartz, pyrophyllite, kaolinite, montmorillonite/muscovite, and chlorite. In the Comstock region the mineral maps show acid-sulfate alteration, widespread propylitic alteration and extensive faulting that offsets the acid-sulfate areas, in contrast to the larger, dominantly acid-sulfate alteration exposed along Geiger Grade. Also, different mineral zones within the intense acid-sulfate areas were mapped. In the Virginia City historic mining district the important weathering minerals mapped include hematite, goethite, jarosite and hydrous sulfate minerals (hexahydrite, alunogen and gypsum) located on mine dumps. Sulfate minerals indicate acidic water forming in the mine dump environment. While there is not an immediate threat to the community, there are clearly sources of acidic drainage that were identified remotely.

Key Words: Imaging spectroscopy, hydrothermal alteration, visible near infrared, short wave infrared, thermal infrared, hyperspectral

*Present address: Jet Propulsion Laboratory, Mail Stop 183-501, 4800 Oak Grove Dr., Pasadena, CA 91109. E-mail, greg.vaughan@jpl.nasa.gov

Vaughan, R. Greg, and Calvin, Wendy M., 2005, Mapping weathering and alteration minerals in the Comstock and Geiger Grade areas using visible to thermal infrared airborne remote sensing data, *in* Rhoden, H.N., Steininger, R.C., and Vikre, P.G., eds., Geological Society of Nevada Symposium 2005: Window to the World, Reno, Nevada, May 2005, p. ###–###.

INTRODUCTION

Location and Geology

The Comstock and Geiger Grade study areas are located in the Virginia Range, in the western part of the Basin and Range geologic province near Reno, Nevada (Fig. 1). The Virginia Range consists mostly of Oligocene to Miocene volcanic rocks that overlie Mesozoic metamorphic rocks (Mzvs) and Cretaceous granodiorite (Kgd) (Whitebread, 1976; Vikre, et al., 1988; Vikre, 1998; Hudson, 2003). Andesite to dacite flows, breccias and intrusions of the Alta Formation (Ta) (18–15 Ma) are overlain by intermediate volcanic, volcaniclastic and locally intrusive rocks of the Kate Peak Formation (Tk) (14.7–12 Ma) (Vikre, 1998; Hudson, 2003) (Fig. 2).

The hydrothermal alteration in rocks exposed along Geiger Grade is characteristic of a magmatic hydrothermal acid sulfate system similar to other alteration zones in the Virginia Range, including the Comstock, Occidental/Flowery, and Jumbo zones near Virginia City, the Washington Hill zone ~15 km to the north of Geiger Grade, and the Gooseberry, Ramsey, and Talapoosa zones in the northeastern Virginia Range (see Vikre 1998). Alteration mineral assemblages in many of these regions have been distinguished based on their dominant mineral constituents (Hudson, 1983; Hudson, 1987; Hutsinpillar and Taranik, 1988; Vikre et al., 1988; Albino, 1991; Vikre 1998; Hudson, 2003). The *alunitic* alteration assemblage consists of alunite + quartz + pyrite; the *alsic* assemblage consists of pyrophyllite + quartz + diaspore; the *kaolinitic* assemblage consists of kaolinite + quartz + pyrite; the *illitic* assemblage consists of illite + montmorillonite (mixed layered) + quartz + pyrite; and the *propylitic* assemblage consists of chlorite + albite + epidote + calcite + illite/sericite + quartz + pyrite. Table 1 lists these alteration assemblages with their characteristic mineralogy and also indicates the minerals that display diagnostic spectral features in the VNIR/SWIR and TIR wavelength regions.

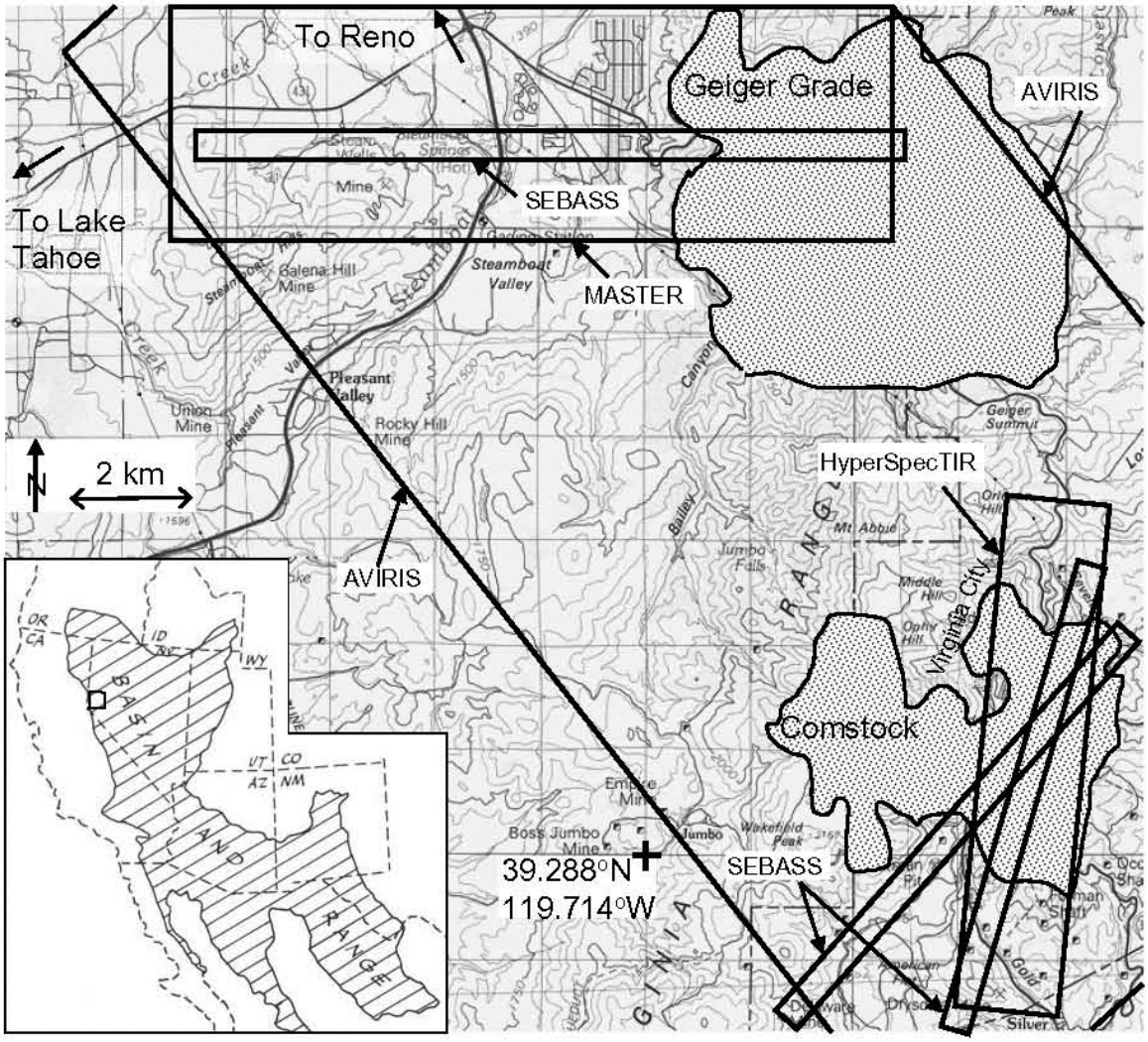

Figure 1. Map showing the location of the study areas with respect to Nevada and the Basin and Range geologic province. Also shown are the outlines of the airborne remote sensing data sets analyzed in this study. Inset figure from Fiero (1986).

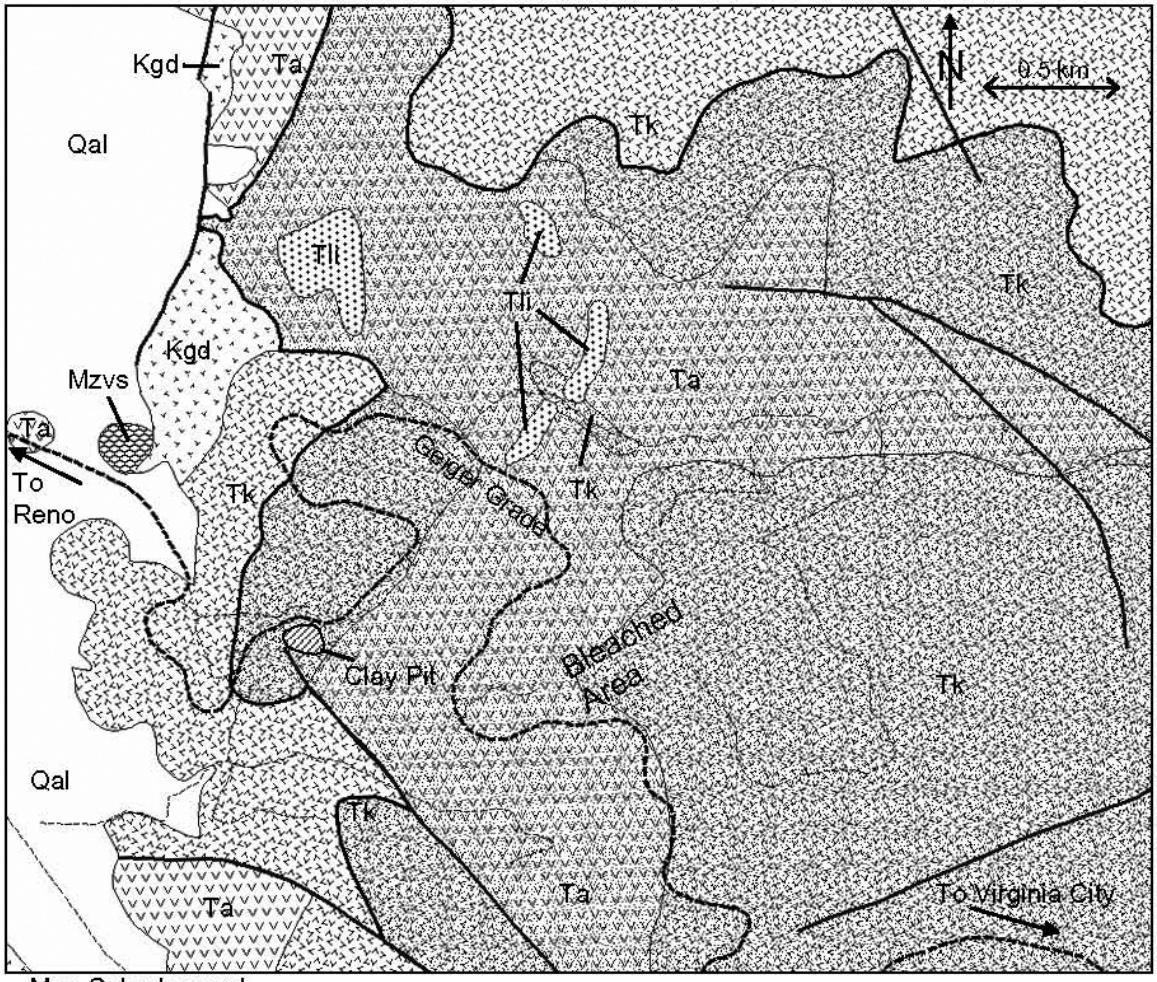

Map Color Legend

Qal	Undifferentiated Alluvial Deposits
	Bleached: Rocks subjected to acid-sulfate type hydrothermal alteration.
Tli	Lousetown Formation: Intrusive plugs and dikes, basaltic to basaltic andesite in composition. 7.4-9.7 Ma in age.
Tk	Kate Peak Formation: Lavas, flow breccias, and porphyritic intrusives. Andesite in composition with hornblende, biotite, and pyroxene. 12-15 Ma (Vikre et al., 1988).
Ta	Alta Formation: Lavas, pyroclastics, and possibly intrusives. Andesite in composition with hornblende and pyroxene. Hydrothermally altered in many areas. 15-20 Ma (Vikre et al., 1988).
Kgd	Granodiorite: Medium-grained granodiorite with Na-plagioclase, microcline, quartz, hornblende, biotite. Late Cretaceous in age.
Mzvs	Gardnerville Formation: Metavolcanic and Metasedimentary Rocks. Triassic? in age.
	Roads
	Faults

Figure 2. Simplified geologic map of Geiger Grade (from Bonham and Bell, 1993).

TABLE 1. ALTERATION MINERAL ASSEMBLAGES IN THE GEIGER GRADE AND COMSTOCK ALTERATION ZONES (from Hudson, 1987).

Alteration Type	Mineral Assemblage	Minerals with diagnostic spectral features in the VNIR/SWIR	Minerals with diagnostic spectral features in the TIR
Alunitic	alunite, quartz, pyrite	alunite	alunite, quartz
Alsic	pyrophyllite, quartz, diaspore, kaolinite, pyrite	pyrophyllite, diaspore, kaolinite	quartz, kaolinite, pyrophyllite
Kaolinitic	kaolinite, quartz, pyrite	kaolinite	kaolinite, quartz
Illitic	illite, quartz, pyrite, montmorillonite	illite, montmorillonite	quartz, illite, montmorillonite
Sericitic	sericite, quartz, pyrite	sericite	sericite, quartz
Propylitic	albite, chlorite, epidote, calcite, illite/sercite, quartz, pyrite	chlorite, epidote, calcite, illite/sercite	albite, chlorite, epidote, quartz illite/sercite, calcite

Virginia City, on the east side of the Virginia Range (Fig. 1), is the home of the historic Comstock mining district and was mined as a source of Au and Ag between 1859 and the 1960's with numerous underground mines and small open pit operations. Figure 3 is a geologic map of the Comstock area simplified from Thompson and White (1964) with some information from Hudson (2003). Hudson (2003) shows a more recent geologic map of a smaller area in the Comstock district with more detail around the Virginia City town site. Re-mapping of the Virginia City quadrangle geology is currently underway (S. Castor, pers. comm. 2004). In the Comstock region, contemporaneous with the Alta Formation was the intrusion of the Davidson diorite (Td) (15.2 Ma), which forms the bulk of Mt. Davidson just west of the Virginia City town site (Hudson, 2003). Hydrothermal alteration in the Comstock district is widespread, with several episodes of hydrothermal events and subsequent precious metal mineralization. Large zones of advanced argillic (acid-sulfate), argillic, and propylitic alteration formed in the region contemporaneous with Alta/Davidson magmatism. Subsequent faulting and high-grade ore mineralization associated with adularia-sericite veins along these structures occurred during younger, low-sulfidation hydrothermal episodes (Castor et al, 2002). Alteration minerals that are exposed in the region include quartz, alunite, kaolinite, pyrophyllite, goethite, hematite, illite/sericite, epidote, albite, mont-morillonite/smectite, and chlorite. The spatial distribution of different mineral assemblages commonly shows a zonation that is related to the location of precious metal deposits (Vikre et al., 1988).

As a historic district with over 100 years of mining, much of the surface area in Virginia City is covered with mine dumps, which commonly contain anomalous concentrations of Hg, As, Cd, Co, Cu, Mo, Ni, Pb, Zn, Se, and Sb. Iron sulfides, most commonly pyrite, exposed at the surface readily oxidize to form secondary Fe-bearing minerals (Swayze et al., 1998; Bigham and Nordstrom, 2000; Montero et al., 2004). Pyrite oxidation is a complex biogeochemical process involving hydration, oxidation, and microbial catalysis that forms acidic water, which can incorporate a large amount of dissolved heavy metals (Bigham and Nordstrom, 2000). As water travels away from the acid-generating source, chemical reactions with other rocks partially neutralize the pH, which leads to the precipitation of Fe-sulfates (like jarosite, or copiapite), Fe-oxyhydroxides (like goethite), and Fe-oxides (like hematite) that sometimes forms a distinct mineral zonation pattern around points of actively oxidizing sulfides (Montero et al., 2004). The occurrence of water-soluble sulfates on mine dumps and tailings is also indicative of acidic surface conditions. These sulfate salts can contain high concentrations of heavy metals in their crystal structure that can be released during increased water flow shortly after rainfall events (Montero et al., 2004). During this study, jarosite was identified forming on the flanks of many of the mine dumps in Virginia City, and hydrous sulfate crusts of hexahydrite, gypsum, alunogen and possibly rozenite were identified as recent precipitates in small depressions on top of some of the weathered dumps. Additionally, a pH of 3.5 was measured in a small puddle on a dump where hexahydrite was found precipitating. Goethite and hematite occur around weathered dumps, and are also nearly ubiquitous in the hydrothermally altered rocks and soils of the surrounding region.

Physical Basis and Background

Primary rock forming minerals as well as many secondary weathering and alteration minerals exhibit wavelength-dependent (spectral) absorption features throughout the visible and infrared wavelength ranges of the electromagnetic spectrum (0.4–25 μm). These features result from the selective absorption of photons with discrete energy levels, and are dependent on the elemental composition, crystal structure, and chemical bonding characteristics of a mineral, and are therefore diagnostic of mineralogy (Hunt, 1980; Clark, 1999). In the region below 1.0 μm, absorption of radiation produces spectral features related to electron transitions within and between atoms, typically in minerals containing iron and other transition metals. In the 8–12 μm range, mineral groups such as silicates, carbonates, sulfates, and phosphates have spectral features related to funda-

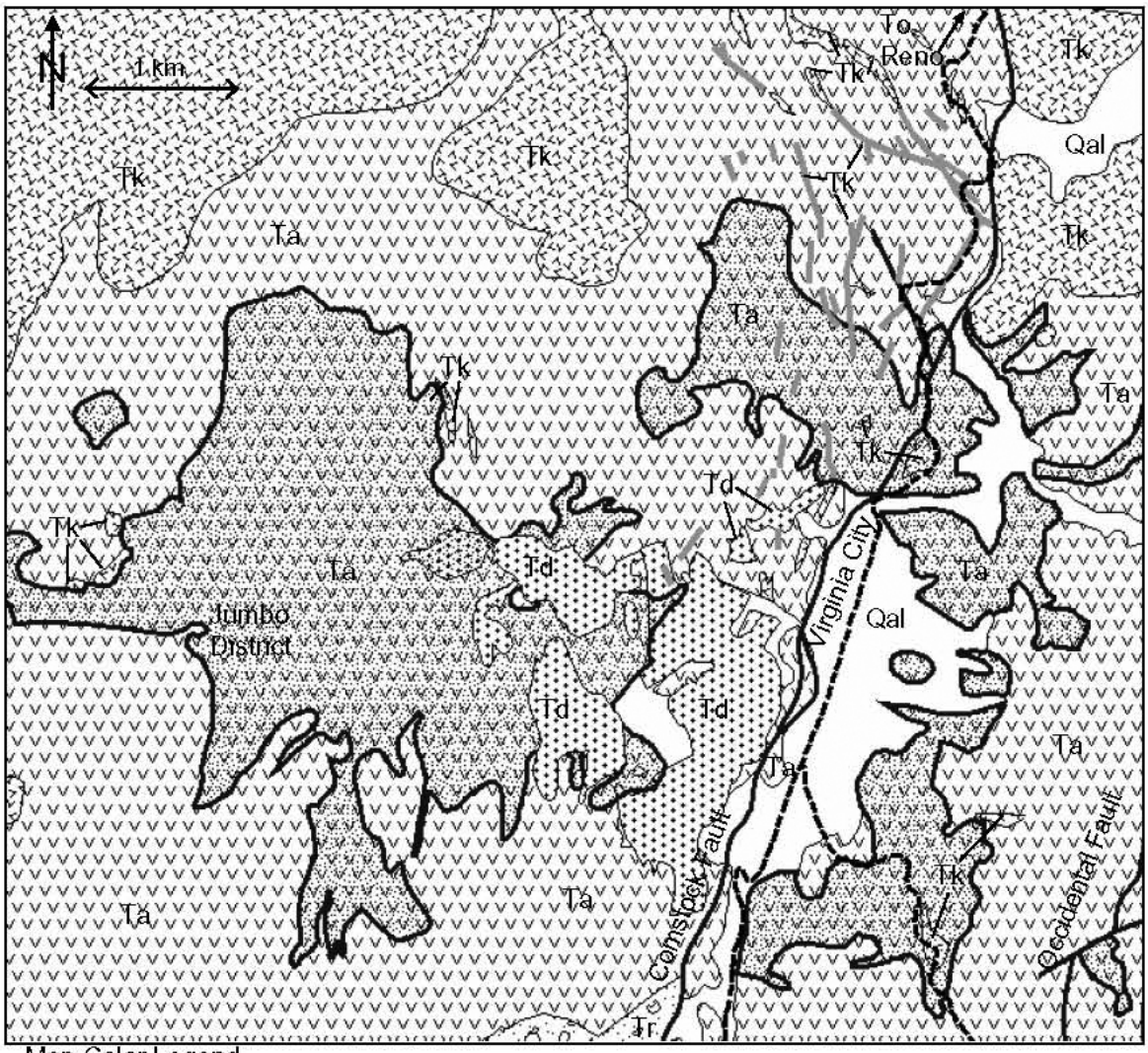

Map Color Legend

Qal	Undifferentiated Alluvial Deposits
	Bleached: Rocks subjected to acid-sulfate type hydrothermal alteration.
Tk	Kate Peak Formation: Lavas, flow breccias, and porphyritic intrusives. Andesite in composition with hornblende, biotite, and pyroxene. 12-15 Ma (Vikre et al., 1988).
Td	Davidson Diorite: Medium-grained intrusive with plagioclase, orthoclase, quartz, and slightly altered ferromagnesian minerals (pyroxene, hornblende, biotite). 15-16 Ma (Vikre et al., 1988)
Ta	Alta Formation: Lavas, pyroclastics, and possibly intrusives. Andesite in composition with hornblende and pyroxene. Hydrothermally altered in many areas. 15-18 Ma (Vikre et al., 1988).
Tr	Hartford Hill Formation: Tuff and tuff breccia with devitrified pumice and glass + quartz, orthoclase, plagioclase and biotite. Rhyolitic in composition.

Roads — Faults — Tk intrusive dikes

Figure 3. Simplified geologic map of the Comstock district and Virginia City (from Thompson and White, 1964; and Hudson, 2003).

mental vibrational frequencies of the interatomic bonds. In the region below 2.5 μm, absorptions due to overtones and combinations of vibrational frequencies occur, and minerals that contain water, hydroxyl, carbonate and sulfate molecules show spectral absorption features. These diagnostic features exhibit measurable variations that allow remote mineral identification.

The identification of a mineral based on its infrared spectrum requires access to the spectra of well-characterized specimens. Thus, the infrared spectral properties for many minerals have been measured in the laboratory, and constitute the empirical basis for the surface mapping applications of infrared remote sensing (Lyon, 1965; Hunt, 1980; Clark et al., 1990; Salisbury et al., 1991; Christensen et al., 2000; Clark et al., 2003). Archives of infrared spectral data for rocks, minerals and vegetation are available for reference from the United States Geological Survey (USGS) spectral library (http://speclab.cr.usgs.gov/index.html), the NASA Jet Propulsion Laboratory (JPL) Advanced Spaceborne Thermal Emission and Reflection Radiometer (ASTER) spectral library (http://speclib.jpl.nasa.gov), and the Arizona State University (ASU) Thermal Emission Spectrometer (TES) spectral library (http://tes.asu.edu/speclib/index.html). Figure 4 shows both VNIR/SWIR (a) and TIR

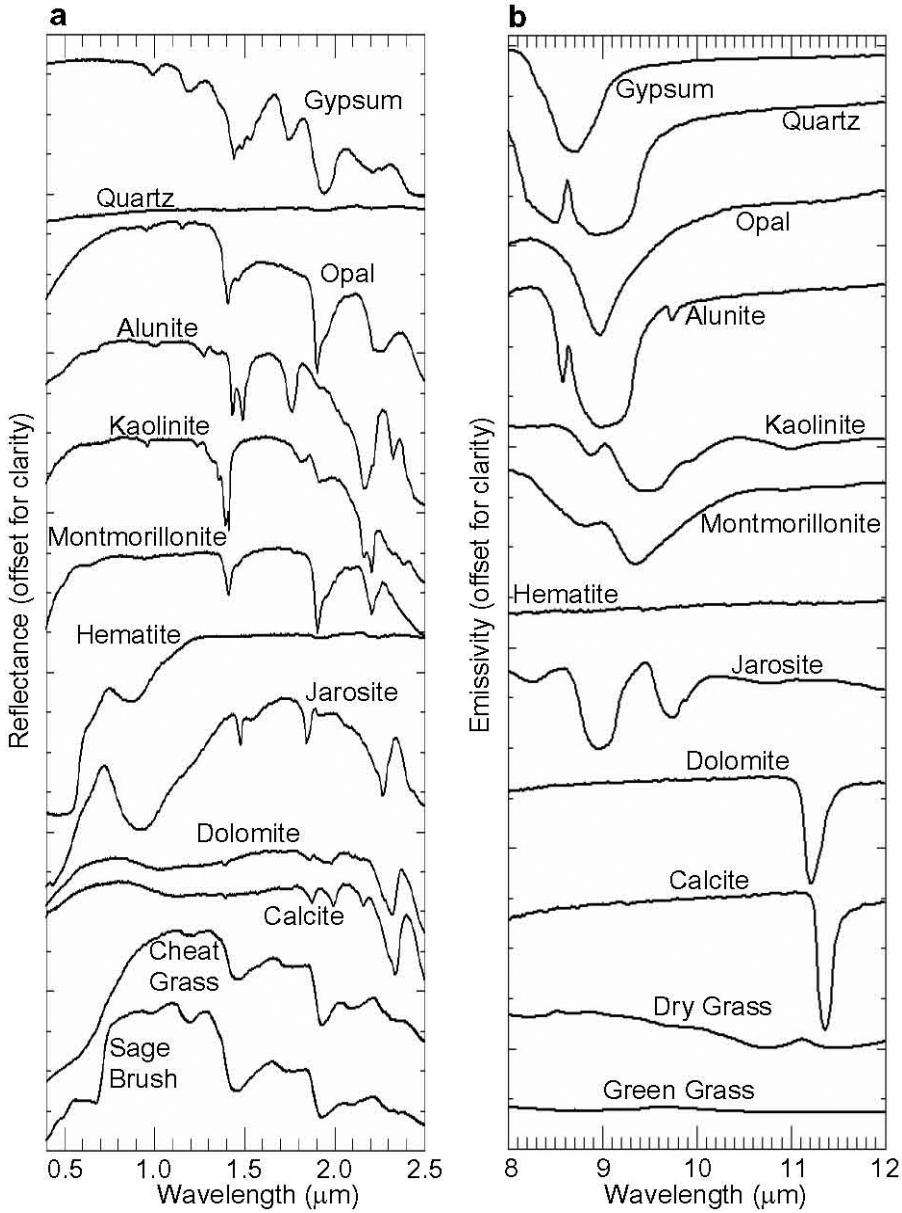

Figure 4. Library reference spectra for minerals and some vegetation common to the case study areas. Both VNIR/SWIR reflectance (a) and TIR emissivity (b) spectra are shown for the same set of materials. The VNIR/SWIR spectra are reproduced from the USGS digital spectral library (speclib05) and the TIR spectra are reproduced from the USGS, ASU and JPL spectral libraries.

(b) reference spectra for minerals, and some vegetation, common to the study areas.

Remote sensing research over the last 30 years has developed a framework for image analysis, processing routines, field calibration and validation of data sets, and established nominal wavelength ranges for surface mineral detection (Abrams et al., 1977; Kahle and Rowan, 1980; Goetz et al., 1983; Marsh and McKeon, 1983; Kahle and Goetz, 1983; Gillespie et al., 1986; Taranik, 1988; Hook et al., 1999; Kruse, 1999; Hook et al., 2001; Cudahy et al., 2000; Rowan and Mars, 2003). Early studies used *multispectral* measurements (i.e. spectral measurements in a few to tens of discontinuous channels) in the VNIR/SWIR range (0.4 to 2.5 μm) to map weathering and alteration minerals (Abrams et al., 1983; Marsh and McKeon, 1983; Podwysocki et al., 1983; Hutsinpillar and Taranik, 1988). With the advent of *hyperspectral* VNIR/SWIR measurements (i.e. spectral measurements in hundreds of narrow, continuous channels) from airborne platforms and better calibration, imaging spectroscopy became possible, and images with high resolution spectral data for each pixel could be directly compared to the reference spectra of pure minerals and used for remote mineral identification (Kruse, 1999; Swayze et al., 1998). For the last 15 years, much research has been focused on the development of image analysis and processing techniques for hyperspectral VNIR/SWIR data, with particular attention to atmospheric correction and unique mineralogical characterization (Vane et al., 1993; King and Clark, 2000; Jacobsen, 2000). There are currently a suite of instruments (summarized in table 2) that acquire hyperspectral imagery in the 0.4 to 2.5 μm wavelength range (Kruse, 1999; Cocks et al., 1998; Watts et al., 2001).

The TIR spectral range (8–12 μm) is also widely used in terrestrial and planetary geologic studies to map surface materials (Kahle and Rowan, 1980; Kahle and Goetz, 1983; Hook et al., 1999; Abrams, 2000). Surface mineral groups that have been mapped using TIR spectral measurements include carbonate, sulfate, phosphate, and felsic vs. mafic silicate minerals (Kahle and Goetz, 1983; Gillespie et al., 1984; Kahle et al., 1988; Sabine et al., 1994; Crowley and Hook, 1996; Ramsey et al., 1999). These studies utilized airborne TIR measurements and prompted the inclusion of multispectral TIR imagers on NASA's recently launched Terra Satellite, including the 1-km spatial resolution Moderate Resolution Imaging Spectroradiometer (MODIS) and the 90-m spatial resolution Advanced Spaceborne Thermal Emission and Reflection Radiometer (ASTER) instruments (Salomonson et al., 1989; Abrams, 2000) (table 2).

New airborne instruments have also been developed (see Table 2), such as the MODIS-ASTER airborne simulator (MASTER) and the Spatially Enhanced Broadband Array Spectrograph System (SEBASS), which are able to make higher spatial and spectral resolution measurements than their airborne predecessors such as the Thermal Infrared Multispectral Scanner (TIMS) (Kahle and Goetz, 1983). As infrared technology has improved, it has paved the way for hyperspectral TIR imaging. This imaging approach has been used for more than a decade in the VNIR/SWIR region, and there are presently a number of relatively new hyperspectral thermal instruments that operate at wavelengths longer than 2.5 μm, including: the Thermal Emission Spectrometer (TES), on the Mars Global Surveyor spacecraft (Christensen, 2000), the Airborne Hyperspectral Imager (AHI) (Lucey et al., 2001), the Spatially Enhanced Broadband Array Spectrograph System (SEBASS) (Hackwell et al., 1996), and an active system (MIRACO$_2$LAS) that uses a CO_2 laser as an IR source (Hook et al. 1998).

Each spectral range (VNIR/SWIR and TIR) has traditionally been treated separately mainly due to the characteristics of detector technology, and differences in the source of radiance (solar reflection vs. thermal emission), which require different approaches to data calibration and processing. The complementary nature of these two wavelength regions has been explored recently by Kruse (2002), Rowan and Mars (2003), and Vaughan (2004). The synthesis of VNIR/SWIR and TIR data provides a way to uniquely identify and map more minerals and mineral assemblages.

INSTRUMENTATION AND DATA PROCESSING

Airborne, Field and Laboratory Measurements

The Airborne Visible Infrared Imaging Spectrometer (AVIRIS) is a hyperspectral imaging spectrometer developed by NASA/JPL. It measures solar reflected radiance in 224 continuous spectral channels between 0.38 and 2.5 μm (Table 2). It has an instantaneous field of view (IFOV) of 1 mrad (0.057°) and a total field of view (TFOV) of 33° (Vane et al., 1993). Data were acquired over Geiger Grade and Virginia City in July 1995 from the ER-2 platform at an altitude of 18 km above ground level (AGL). The images cover a ground swath of about 10.5 km (614 pixels) and have a spatial resolution (pixel size) of ~18 m.

The HyperSpecTIR (HST) is an airborne hyperspectral imaging spectrometer developed and operated by the SpecTIR Corporation. It measures solar reflected radiance in 227 continuous spectral channels between 0.45 and 2.45 μm (Table 2). It has an IFOV of 1 mrad (0.057°) and a TFOV that is selectable from 0 to 1 rad (57°) (Watts et al., 2001). The instrument is mounted on a tilting platform equipped with a "fast optical line-of-sight steering" system that allows for real-time compensation of aircraft motion (roll, pitch and yaw variations) in heavy turbulence, and increases the dwell time over the target (Watts et al., 2001). Images are acquired in a series of overlapping frames rather than a single, continuous strip. HST data were acquired over Virginia City in June 2002 from a Cessna 310 aircraft at an altitude of 2.5 km AGL. The images cover a swath of about 1.1 km and have a spatial resolution of ~2.5 m.

The MODIS-ASTER airborne simulator (MASTER) was designed by the NASA Ames Research Center and JPL to simulate the MODIS and ASTER instruments on board the Terra satellite. It is a multispectral scanner that measures radiance in 50 discontinuous channels between 0.4 and 13 μm (Table 2).

TABLE 2. LABORATORY, FIELD, AIRBORNE AND SPACEBORNE REMOTE SENSING INSTRUMENTS AND SPECTROMETERS.

	Instrument	Spectral Range (μm)	# of Channels	Spectral Band Pass	Spatial Resolution
Field & Lab	ASD[1] FieldSpec	0.4–2.5	2151	3–10 nm	~ 2–14 cm
	JPL Lab FTIR[2]	2.5–15	2256	2 cm^{-1}	~ 1 cm
	ASU Lab FTIR[3]	5–50	840	2 cm^{-1}	~ 1 cm
	D&P[4] μFTIR	5–17	426	4 cm^{-1}	~ 10 cm
Airborne	AVIRIS[5]	0.4–2.5	224	10 nm	4–20 m
	HyperSpecTIR[6]	0.4–2.4	227	5–12 nm	0.5–10 m
	HyMap[7]	0.4–2.5	128	15 nm	2–10 m
	CASI[8]	0.4–1.0	288	2–12 nm	0.5–10 m
	SFSI[9]	1.2–2.4	230	10 nm	0.5–10 m
	MASTER[10]	0.4–2.4	25	40 nm	5–50 m
		3.1–5.2	15	50–60 nm	
		7.8–12.9	10	400–700 nm	
	SEBASS[11]	3.0–5.0	128	2 m	
		7.5–13.5	128	35–65 nm	
	AHI[12]	7.5–11.5	256	100 nm	0.5–10 m
Spaceborne	Hyperion[13]	0.4–2.5	220	10 nm	30 m
	Landsat ETM+[14]	0.5–0.9	1	400 nm	15 m
		0.4–2.4	6	60–350 nm	30 m
		10.4–12.5	1	2100 nm	60 m
	ASTER[15]	0.55–0.81	3	60–100 nm	15 m
		1.65–2.4	6	30–100 nm	30 m
		8.3–11.3	5	350–700 nm	90 m

[1]Analytical Spectral Devices (http://www.asdi.com)
[2]Jet Propulsion Laboratory Fourier Transform Interferometer (http://speclib.jpl.nasa.gov)
[3]Arizona State University Fourier Transform Interferometer (http://tes.asu.edu/speclib)
[4]Designs and Prototypes micro-Fourier Transform Interferometer (http://www.designsandprototypes.com/index.php)
[5]Airborne Visible Infrared Imaging Spectrometer (http://aviris.jpl.nasa.gov)
[6]Spectral Technology and Innovative Research Corporation Hyperspectral Imaging Spectrometer (http://www.spectir.com)
[7]HyVista Corporation Hyperspectral Mapper, developed by Integrated Spectronics (http://www.hyvista.com/main.html and http://www.intspec.com)
[8]Compact Airborne Spectrographic Imager (http://www.itres.com/docs/casi2.html)
[9]SWIR Full Spectrum Imager (http://www.borstad.com/sfsi.html)
[10]MODIS/ASTER Airborne Simulator (http://masterweb.jpl.nasa.gov)
[11]Spatially Enhanced Broadband Array Spectrograph System, developed by Aerospace Corporation (http://www.aero.org)
[12]Airborne Hyperspectral Imager (http://www.higp.hawaii.edu/ahi)
[13]Hyperion (http://eo1.gsfc.nasa.gov/Technology/Hyperion.html)
[14]Landsat Enhanced Thematic Mapper + (http://geo.arc.nasa.gov/sge/landsat/l7.html)
[15]Advanced Spaceborne Thermal Emission and Reflection Radiometer (http://asterweb.jpl.nasa.gov)

There are 25 channels in the VNIR/SWIR range (0.4–2.4 μm), 15 channels in the 3 to 5 μm range, and 10 channels in the TIR (8–12 μm) range. MASTER has an IFOV of 2.5 mrad (0.14°) and a TFOV of 85° (Hook et al., 2001). Data were acquired over Geiger Grade from a KingAir Beachcraft B-200 in September 1999 from an altitude of 2.0 km AGL. The image covers a swath of 3.7 km (716 pixels) and has a spatial resolution of ~5 m.

The Spatially Enhanced Broadband Array Spectrograph System (SEBASS) is an airborne hyperspectral imaging spectrometer designed by Aerospace Corporation. It measures radiance in 128 continuous spectral channels in both the 2.5–5.2, and 7.5–13.5 μm wavelength regions (Table 2). It has an IFOV of 1.1 mrad (0.063°) and a TFOV of 128 mrad (~7.3°) (Hackwell et al., 1996). Data were acquired over Geiger Grade and Virginia City in September 1999 from a flight altitude of 2 km AGL. The images cover a swath of 256 m and have a spatial resolution of ~2 m.

Field sites were used to aid in the calibration of airborne data sets as well as for the validation of the remotely derived mineral maps. The Analytical Spectral Devices (ASD) FieldSpec FR is a field portable spectroradiometer that measures radiance in 2151 channels in the VNIR/SWIR region (0.35–2.5 μm) (Curtiss and Goetz, 1997). It was used in the field for mineral identification and calibration of remote sensing data sets, as well as in the laboratory for high-resolution characterization of field samples. Field spectral data were also collected using a Designs

& Prototypes micro-Fourier Transform Interferometer (μFTIR). The field-portable μFTIR measures radiance between 5 and 17 μm (Hook and Kahle, 1996). Laboratory TIR spectral measurements were made at JPL using a Nicolet 520 FT-IR Spectrometer. Finally, x-ray diffraction (XRD) analyses of bulk rock and mineral separate samples were performed at two different laboratories (the Nevada Bureau of Mines and Geology and the University of Georgia) for mineralogical verification.

Atmospheric Correction of Remote Sensing Data

In the VNIR/SWIR wavelength range, radiance measured at the sensor contains information about surface reflected radiance, the radiance scattered by molecules and aerosols in the atmosphere, and radiance absorbed by atmospheric gases. For the AVIRIS data, the "fast line-of-sight atmospheric analysis of spectral hypercubes" (FLAASH) method was used (Adler-Golden et al., 1998). The FLAASH method uses the latest version of the "moderate resolution atmospheric radiance and transmission" (MODTRAN) model to calculate the atmospheric parameters needed to calculate at-surface reflectance (Berk et al., 1999). For the HST data, in addition to using MODTRAN, an empirical line correction, based on field spectral measurements of natural calibration targets, was used to calculate the at-surface reflectance.

In the TIR wavelength range, radiance measured at the sensor contains information about surface reflected radiance, surface emitted radiance, the radiance emitted by the atmosphere, and atmospheric gas absorption. The MODTRAN model was also used to atmospherically correct MASTER TIR at-sensor radiance to at-surface radiance, and the temperature-emissivity separation (TεS) method described by Gillespie et al. (1998) was used to extract surface emissivity spectra. For the SEBASS data the Aerospace Corporation developed an "In-Scene Atmospheric Compensation" (ISAC) algorithm to correct at-sensor spectral radiance for the effects of atmospheric transmission and path radiance (Young et al., 2002). The corrected at-surface radiance data were then converted to apparent surface emissivity using an emissivity normalization routine (Kealy and Hook, 1993).

Spectral Analysis and Mineral Mapping

Using the full complement of spectral information measured by each instrument, mineral maps were created using a series of hyperspectral data processing methods described by Kruse et al. (2003) and summarized in the flow chart in Figure 5. The first step was the atmospheric correction of at-sensor radiance to at-surface radiance, and extraction of either surface reflectance or emissivity data (described in section 2.2). Spectral data, particularly for hyperspectral data sets, often contain a surplus of information about the surface, as well as remnant noise, so the remaining processing steps serve to minimize noise and focus only on the information that is relevant to characteristic mineralogic features within the image. Pixels with similar spectral patterns were classified together and the spectral features related to the mineral constituents of the pixel were identified by comparison to reference spectra of pure minerals. Finally, the spatial distribution of spectrally mapped minerals was combined with field observations and other maps to generate a mineral map that could be related to the local geology and mineralogic surface expression of the study areas.

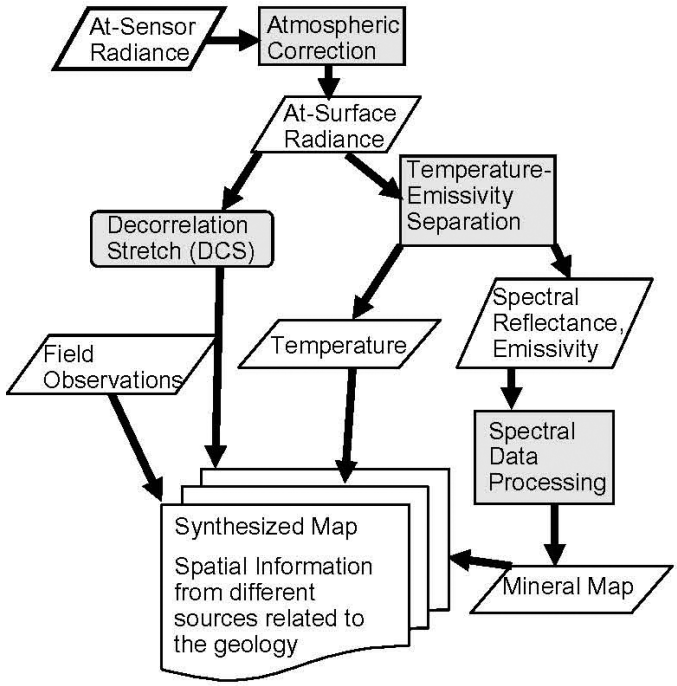

Figure 5. Flow chart illustrating data processing methods. Once the effects of the atmosphere are removed from the radiance measured at the sensor, the at-surface radiance can be enhanced to reveal qualitative information about the surface (DCS), or quantitative temperature, spectral reflectance, or emissivity information can be extracted. The spectral data processing steps serve to minimize noise and focus on information that is relevant to mineralogic features within the image (MNF = minimum noise fraction; PPI = pixel purity index; nDv = n-dimensional visualization; SAM = spectral angel mapper; MF = matched filter).

MINERAL MAPPING RESULTS AND INTERPRETATION

In general, surface cover includes vegetation, water, rock outcrop, soil, or man-made materials such as roofs, roads, and mine dumps. Roofs and other man-made materials sometimes have characteristic spectral features in both VNIR/SWIR and TIR spectral regions, but to focus on mapping minerals related to local geology, pixels over roads and urban areas were not mapped. In some cases pixels were mineralogically homogenous, containing only one mineral phase across the entire pixel. In other cases pixels were mineralogically heterogeneous. A pixel that contains a mixture of different materials produces a spectrum that represents a linear combination of each component. Reference spectra for pure minerals from both VNIR/

SWIR and TIR spectral libraries were mixed together in a linear fashion to approximate the remotely measured spectra and identify the presence of the dominant mixed components. The HST mineral map over a small part of Virginia City (Fig. 6) shows a particularly diverse suite of exposed minerals, including hydrothermal alteration minerals (alunite, kaolinite, pyrophyllite, and montmorillonite/muscovite), as well as a mine dump containing jarosite. The natural color image at the top of Figure 6 is overlain by colored mineral regions keyed to the color legend. Below the map, the accompanying spectral plot shows the remotely measured reflectance spectra for four field sites that are labeled on the map with triangles. Remote, field and

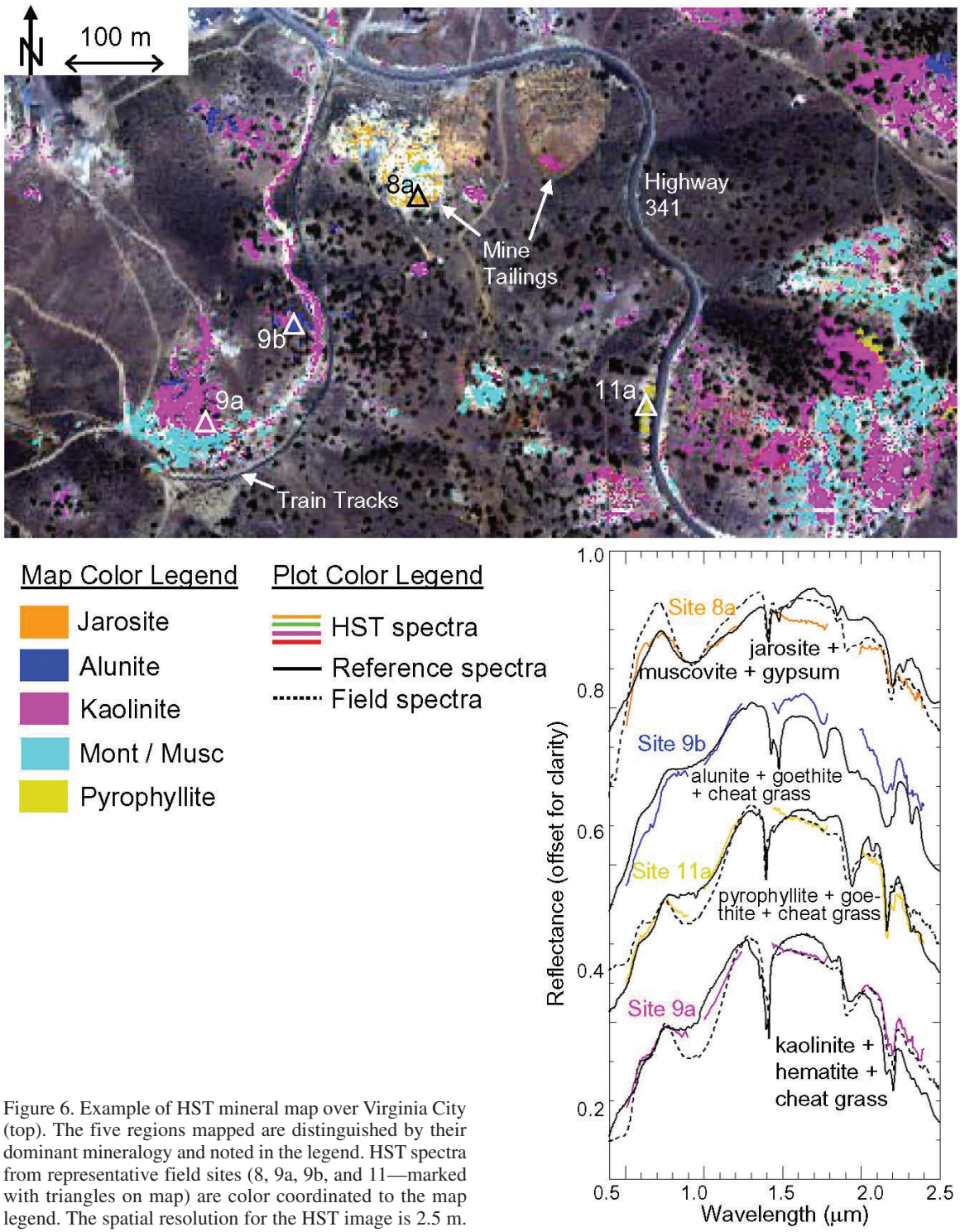

Figure 6. Example of HST mineral map over Virginia City (top). The five regions mapped are distinguished by their dominant mineralogy and noted in the legend. HST spectra from representative field sites (8, 9a, 9b, and 11—marked with triangles on map) are color coordinated to the map legend. The spatial resolution for the HST image is 2.5 m.

laboratory spectra from each site are grouped together for comparison, and each group is offset along the vertical axis to make clear the difference between field sites.

In the spectral plot, the HST spectrum from the mine dump, in orange (site 8a) matches the USGS library reference spectrum for a linear mixture of jarosite (40%), muscovite (45%), and gypsum (15%). The ASD field spectrum matches the HST spectrum and XRD data from field samples indicate the presence of quartz, jarosite, muscovite, and from the sulfate crusts (site 8b), gypsum. The HST spectrum from a resistant outcrop, in blue (site 9b) matches the USGS library reference spectrum for a mixture of alunite (50%), goethite (30%) and cheat grass (20%). XRD data indicate the presence of quartz, Na-alunite, minamiite, and minor kaolinite. The HST spectrum from the talus down hill from a road cut, in dark yellow (site 11a) matches the USGS library reference spectrum for a mixture of pyrophyllite (40%), goethite (40%) and cheat grass (20%). The ASD field spectrum matches the HST spectrum and XRD data indicate the presence of quartz, pyrophyllite, and minor kaolinite. The HST spectrum from an outcrop on a south-facing hill, in magenta (site 9a) matches the USGS library reference spectrum for a mixture of kaolinite (55%), hematite (30%) and cheat grass (15%). The ASD field spectrum matches the HST spectrum and XRD data indicate the presence of quartz and kaolinite.

Instead of showing individual mineral maps from each area, and from each instrument, the following section will show the results of the synthesis of all the mineralogic information derived from each data set.

Hydrothermal Alteration at Geiger Grade and Comstock

The mineral map of the Comstock study area (Fig. 7) shows the distribution of mapped hydrothermal alteration minerals. The colored lines and polygons are overlain on a gray scale digital orthophoto quad (DOQ) image. The geologic units from the map in figure 3 are shown in pale, partly transparent colors. The mineral assemblages mapped using the remote sensing data are shown in solid, opaque colors. Alunitic zones are shown in blue, alsic zones in yellow, kaolinitic zones in magenta, illitic/sericitic zones in cyan, and propylitic zones in green.

Hydrothermal alteration generally falls within the areas mapped as "bleached" on the geologic map of Thompson and White (1964), and is dominated by widespread propylitic and illitic/sericitic zones, notably on the west side (foot wall) of the Comstock fault. Small pods of alunitic, alsic, and kaolinitic alteration occur on the east side (hanging wall) of the Comstock fault around the Virginia City town site. Also, one small alunitic zone and several small kaolinitic zones are mapped in the Jumbo area, and alsic + kaolinitic zones are mapped in the Occidental area in the hanging wall of the Occidental fault. The Davidson diorite (Td) ranges from relatively unaltered to propylitically and illitically altered in some areas. Other propylitic zones occur north of Virginia City close to the Comstock fault, and along the Occidental fault. Hudson (2003) differentiates three different types of propylitic alteration based on the relative abundance of epidote, calcite, and albite in the assemblage. Although these minerals were identified by XRD and spectroscopic methods in the laboratory, the remote mineral maps classify all propylitic alteration together. The center of the Davidson diorite is intensely altered and suggests that this intrusive body was a heat source (and possibly fluid source) for hydrothermal fluid flow during this time. Geochemical data and radioisotope age dates from these rocks support this assumption, but there may have been other acid-sulfate systems associated with later emplacement of small intrusions and dikes associated with Kate Peak volcanism (Vikre, 1998; Castor et al., 2002; Vikre et al., 2003; Hudson, 2003).

The local-scale distribution of alteration mineral zones in part of the Comstock study area is shown in Figure 8. The rocks here are mostly hydrothermally altered andesite of the Alta Formation (Ta), with one small Kate Peak intrusive plug (Tk) in the southeast part of the image. Several small outcrops of alunitic alteration are mapped (dark blue). These quartz + alunite assemblages are more resistant to erosion and commonly form topographic ridges and small pinnacles (see upper photograph). Small resistant pinnacles composed of dominantly quartz + kaolinite (see lower photograph) are also present and look very similar to the quartz + alunite rock. Some of the alunitic zones appear to follow approximately east-west structures, but this has not been confirmed in the field. The alunitic zones grade outward into kaolinitic zones (magenta), and then into illitic/sericitic zones (cyan), which agrees with the model of Hudson (1987). Alsic zones (yellow) rich in pyrophyllite are also mapped with kaolinitic and illitic/sericitic zones (on the east side of the map). These zones are proximal to, and partially contained within, an intermediate-composition intrusive plug (Tk) associated with Kate Peak magmatism. Informally called the lower member of the Kate Peak (Hudson, 2003), these intrusive rocks are also hydrothermally altered throughout the district.

Figure 9 is the mineral map of the Geiger Grade area that combines all of the mineralogic information derived from the remote sensing data sets and field mapping showing the surface minerals related to the mapped hydrothermal alteration zones. The rock units from the geologic map in figure 2 (pale, transparent colors) consist mostly of Alta (Ta) and Kate Peak (Tk) andesite and dacite flows, with some small intrusive plugs of lower Kate Peak and Lousetown Formation basaltic dikes (Tli). Exposures of Mesozoic granodiorite and metamorphic rocks appear in the northwest corner of the map. Alteration mineral zones (opaque colors) generally fall within the area mapped as bleached on the original geologic map. However, there are some alunitic and alsic zones that occur in "unaltered" Kate Peak rocks down a ridge to the west (just south of the SEBASS flight line), indicating that the limit of the bleached area should be extended down this ridge. Similar to the Virginia City mineral maps, there is no differentiation between geologic units; only alteration mineral zones are mapped. In contrast to the Virginia City mineral maps, both the Alta and Kate Peak Forma-

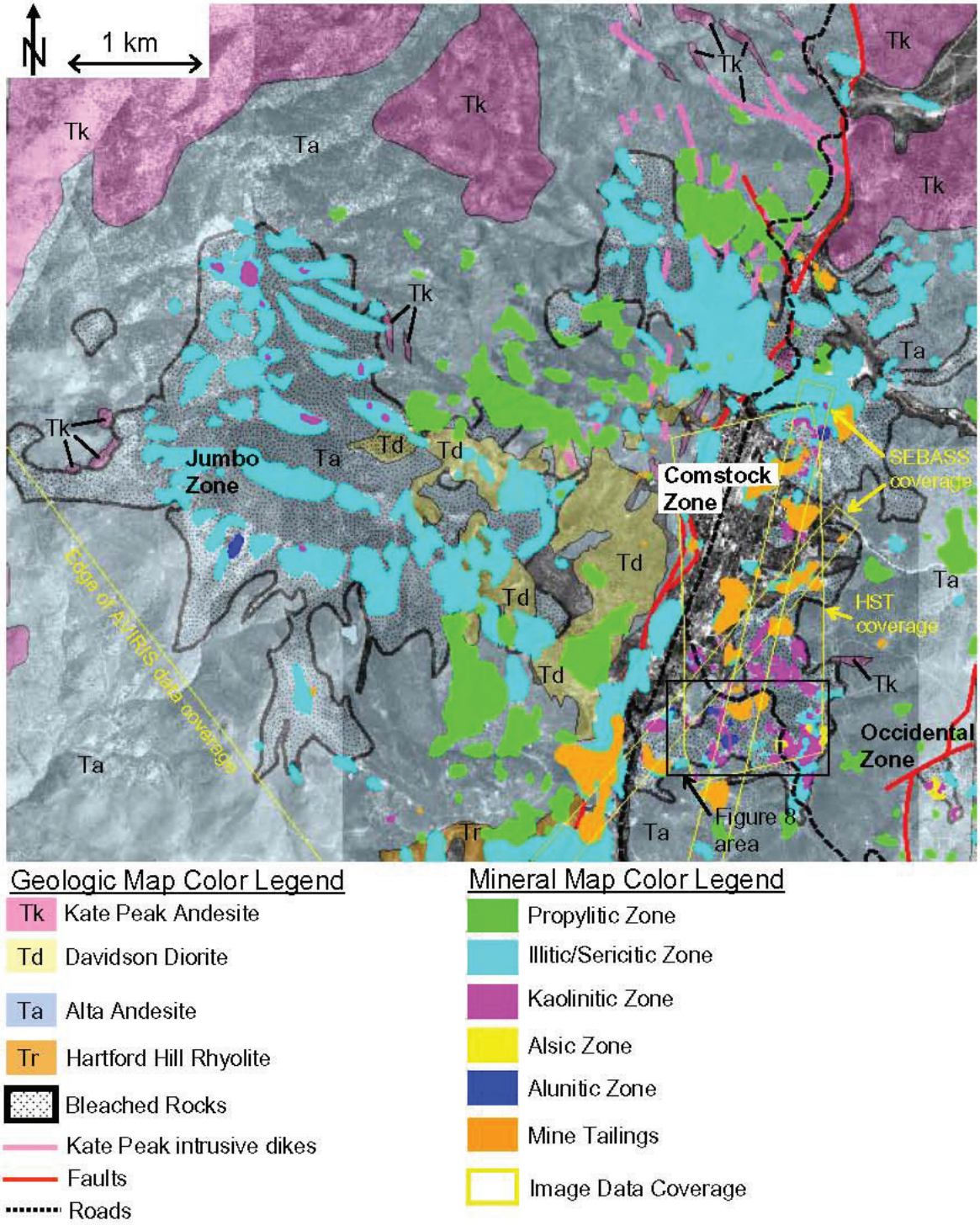

Figure 7. Mineral map of the Comstock district around Virginia City showing the regional-scale distribution of hydrothermal alteration mineral assemblages. The spatial resolution of the DOQ in the background is 1 m.

tions are extensively hydrothermally altered, with no apparent relationship between the type of alteration assemblage and the host rock unit. An $^{40}Ar/^{39}Ar$ radioisotope age of ~13.0 Ma published in Vikre, et al. (2003) for an alunite sample from upper Geiger Grade (southeastern most alunitic area on map) also suggests an acid-sulfate hydrothermal system younger than both Alta and Kate Peak volcanism.

Compared to the Comstock study area, alteration along Geiger Grade is dominated by alunitic and alsic zones, with little or no propylitized rocks. Small propylitized intrusions

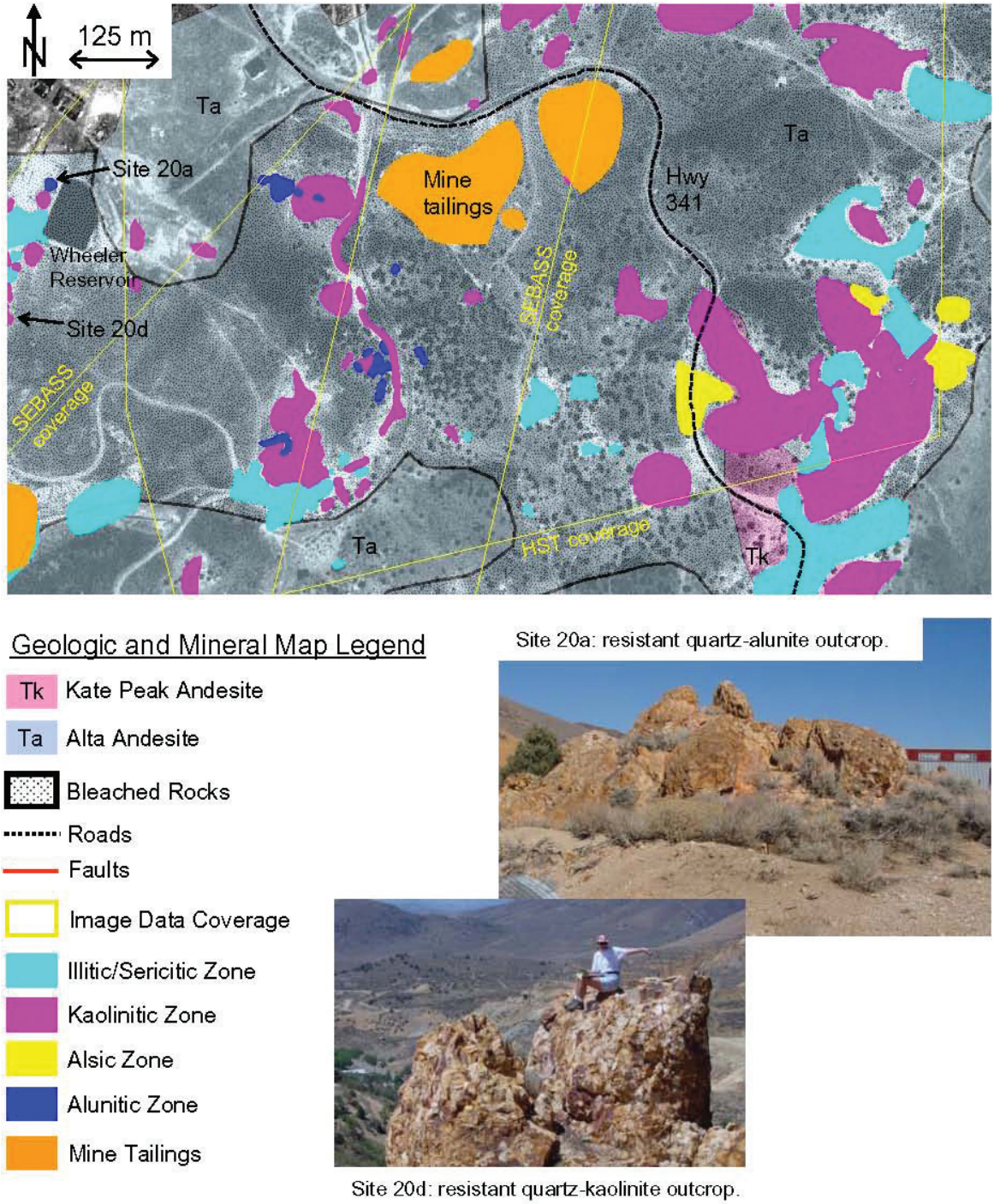

Figure 8. Mineral map of a small area within Virginia City showing the local-scale distribution of hydrothermal alteration mineral assemblages. The spatial resolution of the DOQ in the background is 1 m.

were mapped in the field and there may be larger propylitic zones more distant from the intensely altered areas shown in Figure 9, but overall no significant propylitic zones formed in the Geiger Grade area (unless they have been overprinted by a more recent acid-sulfate system). In the Comstock area propylitic alteration is widespread, and also adjacent to structures along which mineralized adularia-sericite veins are found. Recent research indicates that the pervasive acid-sulfate alteration zones in the Comstock area pre-date ore-grade mineralization along the Comstock and Occidental faults by ~1–2

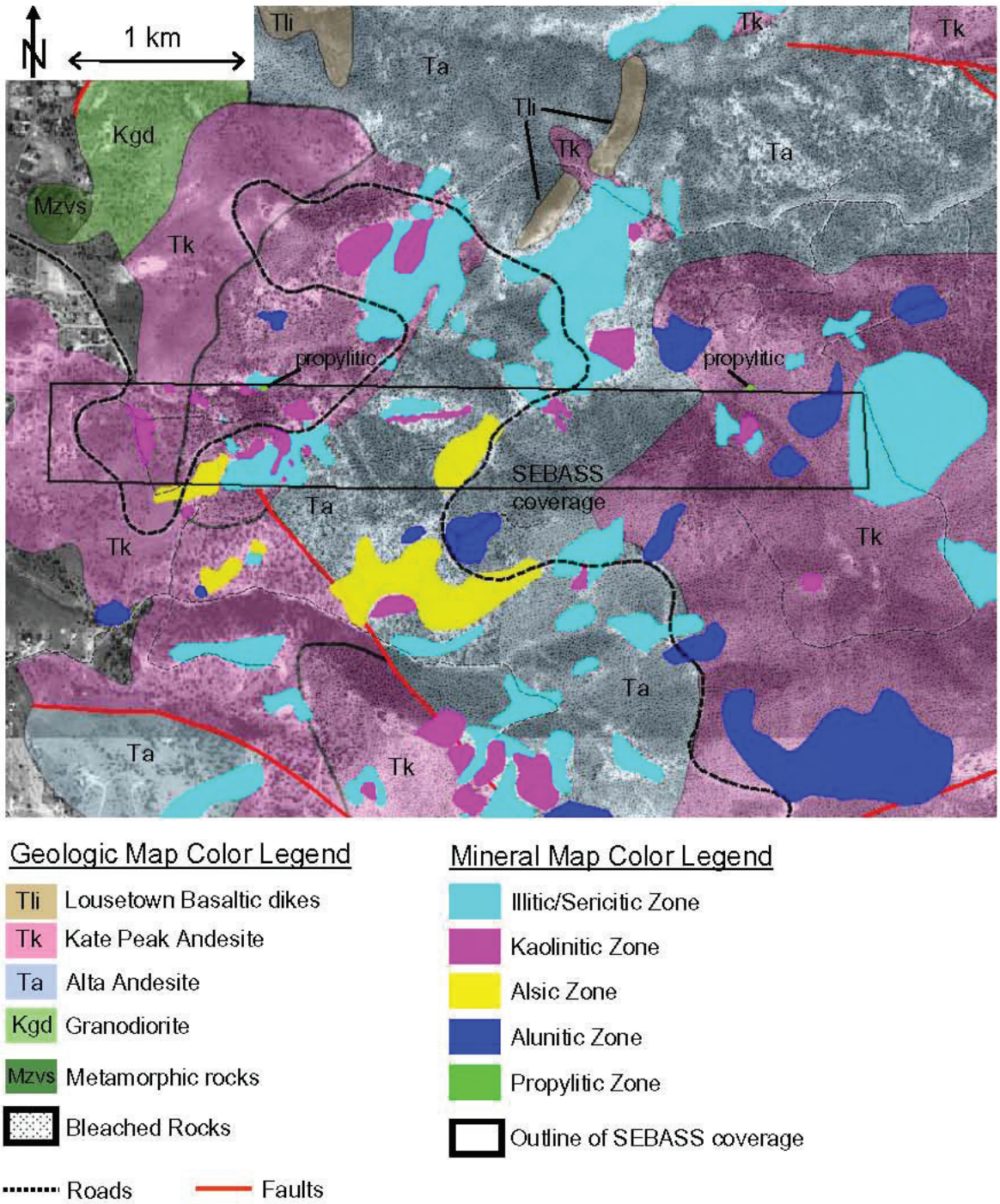

Figure 9. Mineral map of Geiger Grade showing the distribution of acid-sulfate alteration minerals. The extent of the overlapping SEBASS image is outlined in black. The spatial resolution of the DOQ in the background is 1 m.

million years, and bear only incidental spatial relationship to the ore veins (Vikre et al., 1988; Vikre, 1998; Castor et al., 2002; Hudson, 2003).

The spatial distribution of alteration zones appears to be patchy with no obvious structural control, except for one linear east-west kaolinitic zone in the center of the SEBASS swath at Geiger Grade. Also, the predicted progression of alteration zones from alunitic, to alsic, to kaolinitic, to illitic is rarely observed in the surface patterns. In the Comstock district the pervasive acid-sulfate alteration areas were cut by later structures that were subsequently mineralized (Fig. 7), but within intact areas (Fig. 8) only a weak structural control is shown by

the surface zonation patterns. The predicted progression of alteration zones is observed to some degree at a local scale (Fig. 8). Presumably, alteration zonation is more clearly confined by structures at depth. The lack of surface expression for these structures in the remotely derived mineral maps may be related to vertical variations in zonation that complicate the observed lateral patterns. According to Hudson (2003), the low-sulfidation alteration associated with precious metal mineralization followed younger faults, and developed after the acid-sulfate alteration event, but some mineralization did form along faults that were previously the focus of acid-sulfate alteration. Table 3 is a summary of the contrasting characteristics of the Geiger Grade and Comstock alteration zones.

All of the significant base and precious metal deposits in the Virginia Range are located within, or proximal to, acid-sulfate alteration zones in Miocene volcanic rocks (Vikre, 1998). The Comstock region however, appears to be unique. Over a period of ~6 million years multiple episodes of magmatic activity were accompanied by, or followed by, different types of hydrothermal alteration and mineralization. The alteration and mineralization events appear to have shifted from west of Virginia City (Jumbo) to the east (Comstock, then Occidental) with time (Castor et al., 2002; Vikre et al., 2003). Any concentration of precious metals associated with acid-sulfate alteration may have been remobilized during later low-sulfidation hydrothermal events and concentrated in newly-formed structures. Evidence for low-sulfidation alteration, widespread propylitic alteration, or large structures filled with adularia-sericite veins are not found along Geiger Grade. These later processes appear to be unique to the Comstock district and may have been a prerequisite for the formation of a world-class mining district. Other acid-sulfate systems in the Virginia Range that have elevated base and precious metal concentrations have been mined for small amounts of Hg (Washington Hill region) and Au and Ag (Gooseberry, Ramsey and Talapoosa regions) (Vikre, 1998). The proximity of these areas have led some to suggest there may be a large porphyry Cu-Mo deposit at great depths beneath the Virginia Range (Albino, 1991). Regardless, the location of acid-sulfate alteration zones is important for mineral resource exploration potential in the Virginia Range as well as other similar regions.

Mine Dumps in Virginia City

Figure 10 is a mineral map of the Virginia City area showing the distribution of mine dumps, and some open pit exposures, from a combination of the geologic map of Hudson (2003), the Virginia City 7.5 minute topographic map, and from analysis of the DOQ image. Areas that contain jarosite (orange) and the hydrous sulfate minerals gypsum and/or hexahydrite (dark green) were mapped from the remote spectral image data. The yellow lines indicate the extent of high-spatial resolution (SEBASS and HST) data coverage.

Jarosite is indicative of conditions with pH <3 (Montero et al., 2004) and the presence of hydrous Ca-Mg-Al sulfate salts on the surface is indicative of pH values between 3 and 5 (C. Alpers pers. comm., 2004). On top of one dump where both jarosite and hexahydrite were present, a pH of 3.5 was measured in a small puddle formed after a recent rain storm. On the edges of the puddle water, a white sulfate crust of hexahydrite was beginning to precipitate. This field measurement is in agreement with the range of pH values predicted based on the surface mineralogy mapped remotely. Although no known reports of acid mine drainage problems from the Virginia City town site have been published, acid-generating source materials are clearly located within the town site and acidic surface water has been observed after short rainfall events. Of the approximately 0.35 km^2 of mine dumps that are mapped, about 30% contain jarosite mineralization on the surface and about 5% contain water-soluble Mg- and Ca-sulfate salt deposits. To fully evaluate the acid mine drainage potential in Virginia City and relate the composition of sulfate minerals to water chemistry it is important to know the 3-dimensional relationships between the surface, the subsurface fractures within the dumps, and the water table (C. Alpers pers. comm., 2004). Iron-sulfate minerals

TABLE 3. COMPARISON OF THE CHARACTERISTICS OF THE GEIGER GRADE AND COMSTOCK ALTERATION ZONES.

Geiger Grade	Comstock
Both Alta and Kate Peak Formations are intensely altered	Mostly Alta Formation is altered
Possibly multiple pulses of high-sulfidation hydrothermal alteration systems from ~16.0–9.4 Ma	Multiple pulses of both high- and low-sulfidation alteration systems from 18–12 Ma
Dominated by alunitic and alsic assemblages, with some kaolinitic and illitic assemblages, and little to no widespread propylitic assemblages	Dominated by propylitic and illitic/sericitic assemblages
Lack of surface expression that would indicate strong structural control to acid-sulfate alteration zones	Large structures cut acid-sulfate alteration zones and focus low-sulfidation alteration and mineralization; no obvious surface expression of structural control within acid-sulfate zones
Non-economic precious metal mineralization	Economic Ag and Au mineralization concentrated in large structures

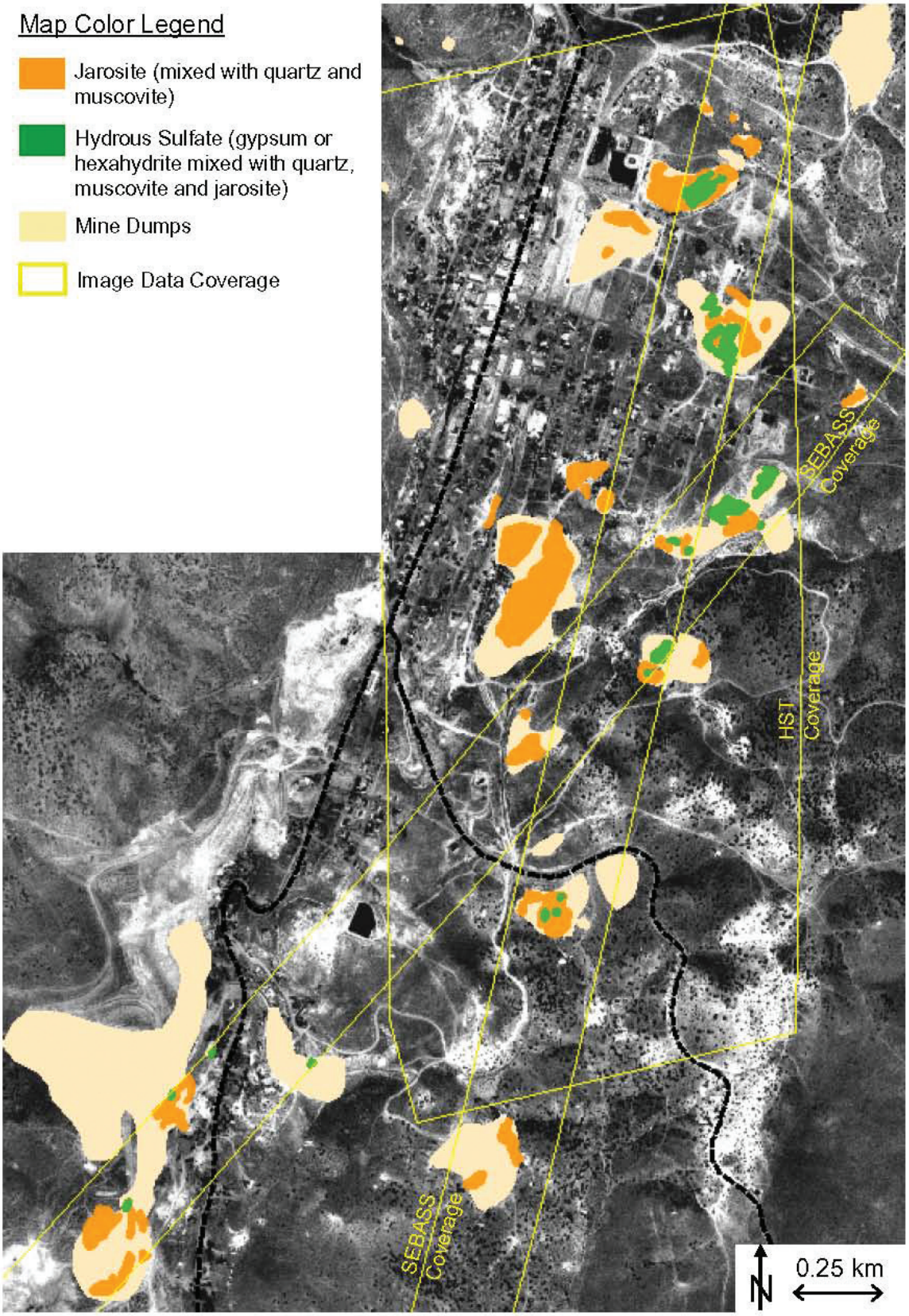

Figure 10. Mineral map of the Virginia City area showing the distribution of mine dumps with jarosite and hydrous sulfate salts. The spatial resolution of the DOQ in the background is 1 m.

like copiapite can be present in the near subsurface and thus not be identified by any remote sensing methods. It is also important to have seasonal data (C. Alpers pers. comm., 2004), particularly in a climate that is variably dry with periodic bursts of wet weather that can radically affect the surface environment. While such additional data shall be relegated to future studies, the remote mineral maps produced in this study indicate the potential for acid mine drainage and possibly heavy metal contamination of ground and surface water.

With respect to the environmental characterization of historic mining areas, jarosite is considered to be the most important mineral to identify to evaluate potential sources of acid mine drainage. Its presence is indicative of oxidizing Fe-sulfide environments and pH conditions of <3 (Montero et al., 2004). The presence of other hydrous sulfate salts (copiapite, hexahydrite, gypsum, rozenite) can also help constrain the chemical characteristics of the water from which they form, but these minerals are very soluble and thus volumetrically minor constituents that may or may not be present at the time of data acquisition. To find soluble sulfate salts on the surface, high-spatial-resolution hyperspectral TIR measurements are best, but the timing has to right. The zoning of goethite and hematite away from oxidizing Fe-sulfide-rich mine dumps that has been observed by others (Montero et al., 2004; Swayze et al., 2000) is of secondary importance because these minerals can be found in many other environments and are not always indicative of acid drainage potential. Mine dumps in Virginia City, while not posing an immediate threat to the community, clearly contain sources of acid drainage. The mineral maps produced in this study have identified these source areas and can help in future reclamation and mitigation efforts should acid mine drainage from Virginia City become a serious problem.

DISCUSSION AND CONCLUSIONS

Hydrothermal Alteration at Geiger Grade and Comstock

The Geiger Grade study area is a large (~8 km^2) magmatic hydrothermal acid-sulfate-type alteration zone characterized by zoned alunitic, alsic, kaolinitic, and illitic mineral assemblages (see Table 1) that occurs within volcanic and intrusive rocks of the Miocene Alta and Kate Peak Formations. The age of this hydrothermal system is not well constrained by radioisotope dating but it is thought to be a result of multiple episodes of hydrothermal alteration between 9.4 and 16 Ma (Vikre et al., 1988). Both Alta and Kate Peak volcanic rocks are intensely altered, and one $^{40}Ar/^{39}Ar$ age from an alunite sample along upper Geiger Grade yielded a date of 13.0 Ma (Vikre et al., 2003). This is approximately contemporaneous with the youngest adularia-sericite vein mineralization event along the Occidental zone in the Virginia City area some 10–12 km away (Castor et al., 2002). These may have been separate hydrothermal systems, or different parts of the same system. The acid-sulfate alteration zone around Virginia City is also thought to be a magmatic hydrothermal system (Vikre et al., 2003), although Hudson (2003) implies that it may be more analogous to the steam-heated system at the Steamboat Springs geothermal area ~15 km to the northwest.

Throughout the Virginia Range acid-sulfate systems are spatially correlated to base and precious metal deposits, however, the Geiger Grade alteration area in different in that it does not contain large propylitic zones and is not known to contain any economic base or precious metal mineralization. In contrast, the Comstock area, mined for Au and Ag, is dominated by large propylitic zones that differ in age from smaller acid-sulfate alteration areas. At least three episodes of magmatism, hydrothermal alteration and precious metal mineralization between 18 and 12 Ma are recorded in the rocks throughout the Comstock mining district around Virginia City. The difference appears to be related to a system of later faults that focused the flow of younger low-sulfidation hydrothermal fluids and mineralized adularia-sericite veins in the Comstock region. The distribution of alteration mineral zones in the Comstock region, and to a lesser degree, the Geiger Grade region, generally agrees with the zonation model of Hudson (1987), however strong structural control is not obvious at the surface.

For mineral resource exploration, identification of these alteration zones is important, particularly the presence of indicator minerals like alunite, pyrophyllite, kaolinite, illite/sericite, and chlorite. These indicator minerals can be identified by either VNIR/SWIR or TIR hyperspectral data, but clay minerals are more easily separated using VNIR/SWIR wavelengths. In other mineral resource exploration applications, the identification of quartz is also important, necessitating the use of hyperspectral TIR image data.

Acid Rock Drainage Potential in Virginia City

The historic Comstock mining district around Virginia City has about 1 km^2 of exposed mine dumps, approximately 30% of which are covered with jarosite, indicative of active acid-generating processes. Hydrous Ca-Mg-sulfate minerals such as gypsum and hexahydrite are also found on weathered mine dumps and indicate slightly acidic conditions. Lack of acid-indicator minerals away from the, dumps may indicate that the buffering capacity of surrounding rocks is enough to confine acidic conditions to the mine dump environment. Although there are studies of Hg flux from mill tailings at the base of six-mile canyon east of Virginia City (Fenstermaker and Miller, 1994), to date there are no known reports of acid mine drainage from Virginia City mine dumps. However, there are clearly sources of acid rock drainage present in Virginia City and the presence of minerals within dumps indicative of more acidic conditions can not be ruled out; further geochemical surveys will be necessary to fully evaluate the potential for acid mine drainage from Virginia City. Remote sensing for environmental site characterization requires high-spatial resolution imagery (to identify small source regions on mine

dumps), and both VNIR/SWIR and TIR hyperspectral measurements (to identify all the possible acid-indicator minerals, which are typically sulfates). Although this study has contributed some new mineral spectra for reference, there needs to be a more comprehensive set of sulfate mineral reference spectra for effective remote mineral identification.

Remote Sensing Technology

Multi-channel infrared remote sensing tools can be used to identify and map weathering and alteration minerals that are characteristic of hydrothermal systems as well as acid mine drainage potential. For remote mineral resource exploration applications, hyperspectral VNIR/SWIR measurements with a spatial resolution of 5–20 m and a swath between 10 and 20 km are ideal. For environmental site characterization, 1–2 m spatial resolution hyperspectral VNIR/SWIR and TIR measurements with a 2–5 km swath are ideal.

Given these examples of the advantages of high spatial and high spectral resolution measurements, and the utility of combining image data from multiple wavelength regions, this research should be helpful in placing some limits on, and setting some goals for, the specifications of future airborne and spaceborne remote sensing systems for geological applications. Currently the spaceborne instrument, ASTER, is acquiring multispectral VNIR/SWIR and TIR image data with 15 to 90 m spatial resolution, and Hyperion is a spaceborne hyperspectral VNIR/SWIR imaging spectrometer with 30 m spatial resolution. Wide-swath, low-spatial resolution images are beneficial for global and regional mapping if the spectral resolution is high enough to detect sub-pixel mineral components, and if the signal-to-noise ratio is high enough to differentiate unique spectral signatures from inherent system noise. Such limitations do not diminish the importance of spaceborne remote sensing systems, but emphasize the necessity of airborne instruments to fill a niche for local to intermediate scale study areas (1x1 to 10x10 km^2). The next advance in geologic remote sensing tools from either air or space should combine the advantages of high spatial resolution, wide swath, high spectral resolution and high signal-to-noise ratio with measurements in both VNIR/SWIR and TIR spectral regions.

ACKNOWLEDGEMENTS

The research described in this paper was carried out in part at the Jet Propulsion Laboratory (JPL), California Institute of Technology, under contract with the National Aeronautics and Space Administration (NASA) as part of the Earth Observing System Mission to Planet Earth Program. This work has also been supported by the Nevada Space Grant Consortium, the Arthur Brant Laboratory for Exploration Geophysics, and NASA grant NGT5-50362 (the NASA Graduate Student Research Program Fellowship). The authors would like to thank John Hackwell and Patricia Lew at Aerospace Corporation for the opportunity to participate in the 1999 SEBASS group shoot and for helping with raw data reduction and implementation of the ISAC routine. Also, many thanks to Cindy Grove and Ron Alley at JPL for providing some TIR laboratory measurements of field samples and the atmospheric profile data for MASTER data calibration; Mario Desilets at the Nevada Bureau of Mines and Geology, and Paul Schroeder at the University of Georgia for assistance with XRD analyses of field samples; Steve Castor at the Nevada Bureau of Mines and Geology and Peter Vikre at the USGS for helpful insights into Virginia City's geology; Richard Bedell, Joe Polovina and an anonymous reviewer for helpful comments about this manuscript; and finally the AVIRIS team at JPL and the SpecTIR Corporation for providing hyperspectral data sets for geologic analysis.

REFERENCES

Abrams, M.J., Ashley, R.P., Rowan, L.C., Goetz, A.F.H. and Kahle, A.B. (1977). Mapping of Hydrothermal Alteration Minerals in the Cuprite Mining District, Nevada, Using Aircraft Scanner Images for the Spectral Region 0.46 to 2.36 μm. *Geology*, 5, p. 713–718.

Abrams, M.J., Brown, D., Lepley, L. and Sadowski, R. (1983). Remote Sensing for Porphyry Copper Deposits in Southern Arizona. *Economic Geology*, 78 (4), p. 591–604.

Abrams, M.J. (2000). The Advanced Spaceborne Thermal Emission and Reflection Radiometer (ASTER): Data Products for the High Resolution Imager on NASA's Terra Platform. *International Journal of Remote Sensing*, 21 (5), p. 847–859.

Adler-Golden, S., Berk, A., Bernstein, L.S., Richtsmeier, S.C., Acharya, P.K., and Matthew, M.W. (1998). FLAASH, A MODTRAN 4 Atmospheric Correction Package for Hyperspectral Data Retrievals and Simulation. *Proceedings of the 7th JPL Airborne Earth Science Workshop*, JPL.

Albino, G.V. (1991). Geology and Mineral Deposits of the Virginia Range, Washoe, Lyon, and Storey Counties, Nevada. Geological Society of Nevada 1992 Spring Field Trip 2 Guidebook, Special Publication #15, p.146–154.

Berger, B.R., Tingley, J.V., and Drew, L.J. (2003). Structural Localization and Origin of Compartmentalized Fluid Flow, Comstock Lode, Virginia City, Nevada. *Economic Geology*, 98, p. 387–408.

Berk, A., Anderson, G.P., Bernstein, L.S., Acharya, P.K., Dothe, H., Matthew, M.W., Adler-Golden, S., Chetwynd, J.H. Jr., Richtsmeier, S.C., Pukall, B., Allred, C.L., Jeong, L.S., and Hoke, M.L. (1999). MODTRAN4 Radiative Transfer Modeling for Atmospheric Correction. *Proceedings of the 8th JPL Airborne Earth Science Workshop*, JPL Publication 99-17.

Bigham, J.M. and Nordstrom, D.K. (2000). Iron and Aluminum Hydroxysulfates from Acid Sulfate Waters. Ch 7 in: *Reviews in Mineralogy and Geochemistry*, *v. 40, Sulfate Minerals: Crystallography, Geochemistry, and Environmental Significance*, C.N. Alpers, J.L. Jambor, and D.K. Nordstrom editors, Mineralogical Society of America, Washington, D.C., p. 351–403.

Bonham, H.F., Jr. and Bell, J.W. (1993). Geologic Map of the Steamboat quadrangle, Nevada. Nevada Bureau of Mines and Geology, Map 4Fg.

Castor, S.B., Garside, L.J., Henry, C.D., Hudson, D.M., McIntosh, W.C., and Vikre, P.G. (2002). Multiple Episodes of Magmatism and Mineralization in the Comstock District, Nevada. *Abstracts with Programs*, Geological Society of America, 34 (6), p. 185.

Christensen, P.R. (2000). Introduction to the Special Section: Mars Global Surveyor Thermal Emission Spectrometer. *Journal of Geophysical Research*, 105 (E4), p. 9507.

Christensen, P.R., Bandfield, J.L., Hamilton, V.E., Howard, D.A., Lane, M.D., Piatek, J.L., Ruff, S.W., and Stefanov, W.L. (2000). A Thermal Emis-

sion Spectral Library of Rock-Forming Minerals. *Journal of Geophysical Research*, 105 (E4), p. 9735–9739.

Clark, R.N., King, T.V.V., Klejwa, M., and Swayze, G.A. (1990). High Spectral Resolution Reflectance Spectroscopy of Minerals. *Journal of Geophysical Research*, 95 (B8), p. 12653–12680.

Clark, R.N. (1999). Spectroscopy of Rocks and Minerals and Principles of Spectroscopy. Ch 1 in: *Remote Sensing for the Earth Sciences: Manual of Remote Sensing*, A.N. Rencz editor, 3rd edition, vol. 3, John Wiley & Sons, New York.

Clark, R.N., Swayze, G.A., Wise, R., Livo, K.E., Hoefen, T.M., Kokaly, R.F., and Sutley S.J. (2003). USGS Digital Spectral Library splib05a. *USGS Open File Report*, 03-395.

Cocks T., Jenssen, R., Stewart, A., Wilson, I., and Shields T. (1998). The HyMap Airborne Hyperspectral Sensor: The System, Calibration and Performance. In: *Proceedings of 1st EARSeL Workshop on Imaging Spectroscopy*, M. Schaepman, D. Schläpfer, and K.I. Itten, editors, p. 37–43.

Crowley, J.K. and Hook, S.J. (1996). Mapping Playa Evaporite Minerals and Associated Sediments in Death Valley, CA, with Multispectral Thermal Infrared Images. *Journal of Geophysical Research*, 101 (B1), p. 643–660.

Cudahy, T.J., Okada, K., Yamato, Y., Maekawa, M., Hackwell, J.A., and Huntington, J.F. (2000). Mapping Skarn and Porphyry Alteration Mineralogy at Yerington, Nevada, Using Airborne Hyperspectral TIR SEBASS Data. *CSIRO Exploration and Mining Report 734R*, CSIRO Exploration and Mining Co., Floreat Park, WA, Australia.

Curtiss, B. and Goetz, A.F.H. (1997). Field Spectrometry: Techniques and Instrumentation. *Analytical Spectral Devices FieldSpec™ User's Guide*, Appendix A, p. 45–62.

Fenstermaker, L.K. and Miller, J.R. (1994). Identification of Fluvially Redistributed Mill Tailings Using High Spectral Resolution Aircraft Data. *Photogrammetric Engineering & Remote Sensing*, 60 (8), p. 989–995.

Fiero, B. 1986. *Geology of the Great Basin*. University of Nevada Reno Press, Reno, NV.

Gillespie, A.R., Kahle A.B., and Palluconi, F.D. (1984). Mapping Alluvial Fans in Death Valley, CA, Using Multispectral Thermal Infrared Images. *Geophysical Research Letters*, 11 (11), p. 1153–1156.

Gillespie, A.R., Kahle A.B., and Walker, R.E. (1986). Color Enhancement of Highly Correlated Images. I. Decorrelation and HIS Contrast Stretches. *Remote Sensing of Environment*, 20, p. 209–235.

Goetz, A.F.H., Rock, B.N. and Rowan, L.C. (1983). Remote Sensing for Exploration: An Overview. *Economic Geology*, 78 (4), p. 573–590.

Goetz, A.F.H, Vane, G., Solomon, J.E., and Rock, B.N. (1985). Imaging Spectrometry for Earth Remote Sensing. Science, 228 (4704), p. 1147–1152.

Hackwell, J.A., Warren, D.W., Bongiovi, R.P., Hansel, S.J., Hayhurst, T.L., Mabry, D.J., Sivjee, M.G., and Skinner, J.W. (1996). LWIR/MWIR Imaging Hyperspectral Sensor for Airborne and Ground-based Remote Sensing. *SPIE*, 2819, p. 102–107.

Hook, S.J. and Kahle, A.B. (1996). The Micro Fourier Transform Interferometer (μFTIR)—A New Field Spectrometer for Acquisition of Infrared Data of Natural Surfaces, *Remote Sensing of Environment*, 56, p. 172–181.

Hook, S. J., Cudahy, T. J., Kahle, A. B., and Whitbourn, L.B. (1998). Synergy of Active and Passive Airborne Thermal Infrared Systems for Surface Compositional Mapping. *Journal of Geophysical Research*, 103, p. 18269–18276.

Hook, S.J., Abbott, E.A., Grove, C., Kahle, A.B., and Palluconi, F.D. (1999). Use of Multispectral Thermal Infrared Data in Geological Studies. Ch 2 in: *Remote Sensing for the Earth Sciences: Manual of Remote Sensing*, A.N. Rencz editor, 3rd edition, vol. 3, John Wiley & Sons, New York.

Hook, S.J., Myers, J., Thome, K.J., Fitzgerald, M., and Kahle, A.B. (2001). The MODIS/ASTER Airborne Simulator (MASTER)—A New Instrument for Earth Science Studies. *Remote Sensing of Environment*, 76, p. 93–102.

Hudson, D.M. (1983). Alteration and Geochemical Characteristics of the Upper Parts of Selected Porphyry Systems, Western Nevada. *Ph.D. Thesis*, University of Nevada, Reno.

Hudson, D.M. (1987). Steamboat Springs Geothermal Area, Washoe County, Nevada. In: *Bulk Mineable Precious Metal Deposits of the Western United States*, J.L. Johnson editor, Geological Society of Nevada field trip guidebook, p. 408–412.

Hudson, D.M. (2003). Epithermal Alteration and Mineralization in the Comstock District, Nevada. *Economic Geology*, 98, p. 367–385.

Hutsinpiller, A. and Taranik, J.V. (1988). Spectral Signatures of Hydrothermal Alteration at Virginia City, Nevada. In: Bulk Mineable Precious Metal Deposits of the Western United States, Robert W. Schafer editor, Geological Society of Nevada Symposium Proceedings, p. 505–530.

Hunt, G.R. (1980). Electromagnetic Radiation: The Communication Link in Remote Sensing. Ch 2 in: *Remote Sensing in Geology*, B.S. Siegal and A.R Gillespie editors, John Wiley, New York, p. 5–45.

Jacobsen, A., Heidebrecht, K.B., and Goetz, A.F.H. (2000). Assessing the Quality of the Radiometric and Spectral Calibration of *casi* Data and Retrieval of Surface Reflectance Factors. *Photogrammetric Engineering and Remote Sensing*, 66 (9), p. 1083–1091.

Kahle, A.B. and Rowan, L.C. (1980). Evaluation of Multispectral Middle Infrared Aircraft Images for Lithologic Mapping in the East Tintic Mountains, Utah. *Geology*, 8, p. 234–239.

Kahle, A.B. and Goetz, A.F. (1983). Mineralogic Information from a New Airborne Thermal Infrared Multispectral Scanner. *Science*, 222, p. 24–27.

Kahle, A.B., Gillespie, A.R., Abbott, E.A., Abrams, M.J., Walker, R.E., Hoover, G., and Lockwood, J.P. (1988). Relative Dating of Hawaiian Lava Flows Using Multispectral Thermal Infrared Images: A New Tool for Geologic Mapping of Young Volcanic Terrains. *Journal of Geophysical Research*, 93 (B12), p. 15239–15251.

Kealy, P.S. and Hook, S.J. (1993). Separating Temperature and Emissivity in Thermal Infrared Multispectral Scanner Data: Implications for Recovery of Land Surface Temperatures. *IEEE Transactions on Geoscience and Remote Sensing*, 31, p. 1155–1164.

King, T.V.V. and Clark, R.N. (2000). Verification of Remotely Sensed Data. Ch 5 in: *Remote Sensing for Site Characterization*, F. Kuehn, T. King, B. Hoerig, and D. Peters editors, Springer-Verlag, Berlin, Germany.

Kirkland, L., Herr, K., Keim, E., Adams, P., Salisbury, J., Hackwell, J., and Treiman, A. (2001). First Use of an Airborne Thermal Infrared Hyperspectral Scanner for Compositional Mapping. *Remote Sensing of Environment*, 80, p. 447–459.

Kruse, F.A. (1999). Visible-Infrared Sensors and Case Studies. Ch 11 in: *Remote Sensing for the Earth Sciences: Manual of Remote Sensing*, A.N. Rencz editor, 3rd ed. vol. 3, John Wiley & Sons, New York.

Kruse, F.A. (2002). Combined SWIR and LWIR Mineral Mapping Using MASTER/ASTER. In: Proceedings, IGARSS 2002, CD ROM, Toronto, Canada, p. 2267–2269.

Kruse, F.A., Boardman, J.W. and Huntington, J.F. (2003). Comparison of Airborne Hyperspectral Data and EO-1 Hyperion for Mineral Mapping. In: *Special Issue, IEEE Transactions on Geoscience and Remote Sensing*, 41 (6), p. 1388–1400.

Lucey, P.G., Williams, T.J., Hinrichs, J. L., Winter, M.E., Steutel, D., and Winter, E.M. (2001). Three years of operation of AHI: the University of Hawaii's Airborne Hyperspectral Imager. In: *Proceedings SPIE Infrared Technology and Applications XXVII*, B.F. Andresen, G.F. Fulop, and M. Strojnik editors, vol. 4369, p. 112–120.

Lyon, R.J.P. (1965). Analysis of Rocks by Spectral Infrared Emission (8 to 25 microns). *Economic Geology*, 60, p. 715–736.

Marsh, S.E. and McKeon, J.B. (1983). Integrated Analysis of High-Resolution Field and Airborne Spectroradiometer Data for Alteration Mapping. *Economic Geology*, 78 (4), p. 618–632.

Montero, I.C., Brimhall, G.H., Alpers, C.N., and Swayze, G.A. (2004). Characterization of Waste Rock Associated with Acid Drainage at the Penn Mine, California, by Ground-based Visible to Short-wave Infrared Reflectance Spectroscopy Assisted by Digital Mapping. *Chemical Geology*, in review.

Podwysocki, M.H., Segal, D.B., and Abrams, M.J. (1983). Use of Multispectral Scanner Images for Assessment of Hydrothermal Alteration in the Marysvale, Utah, Mining Area. *Economic Geology*, 78 (4), p. 573–590.

Ramsey, M.S., Christensen, P.R., Lancaster, N., and Howard, D.A. (1999). Identification of Sand Sources and Transport Pathways at the Kelso

Dunes, California, Using Thermal Infrared Remote Sensing. *GSA Bulletin*, 111 (5), p. 646–662.

Rowan, L.C. and Mars, J.C. (2003). Lithologic Mapping in the Mountain Pass, California Area Using Advanced Spaceborne Thermal Emission and Reflection Radiometer (ASTER) Data. *Remote Sensing of Environment*, 84, p. 350–366.

Sabine, C., Realmuto, V.J., and Taranik, J.V. (1994). Quantitative Estimation of Granitoid Composition from Thermal Infrared Multispectral Scanner (TIMS) data, Desolation Wilderness, Northern Sierra Nevada, California. *Journal of Geophysical Research*, 99 (B3), p. 4261–4271.

Salisbury, J.W., Walter, L.S., Vergo, N., and D'Aria, D.M. (1991). *Infrared (2.1–25 μm) Spectra of Minerals*. Johns Hopkins University Press, Baltimore, MD.

Salomonson, V., Barnes, W., Maymon, P., Montgomery, H., and Ostrow, H. (1989). MODIS: Advanced Facility Instrument for Studies of the Earth as a System. *IEEE Transactions on Geoscience and Remote Sensing*, 27 (4), p. 145–153.

Swayze, G.A., Clark, R.N., Smith, K.S., Hageman, P.L., Sutley, S.J., Pearson, R.M., Rust, R.S., Briggs, P.H., Meier, A.L., Singleton, M.J., and Roth, S. (1998). Using Imaging Spectroscopy to Cost-Effectively Locate Acid-Generating Minerals at Mine Sites: An Example From the California Gulch Superfund Site in Leadville, Colorado. Proceedings of the 7th Airborne Earth Science Workshop, JPL publication 97-21 (1), p. 385–389.

Swayze, G.A., Smith, K.S., Clark, R.N., Sutley, S.J., Pearson, R.M., Vance, J.S.,. Hugeman, P.L, Briggs, P.H., Meier, A.L., Singleton, M.J., Roth, S. (2000). Using Imaging Spectroscopy to Map Acidic Mine Waste. Environ. Sci. Technol. 34, 47–54.

Taranik, J.V. (1988). Application of Aerospace Remote Sensing Technology to Exploration for Precious Metal Deposits in the Western United States. In: *Bulk Mineable Precious Metal Deposits of the Western United States*, Robert W. Schafer editor, GSN Symposium Proceedings, Geological Society of Nevada, Reno, NV.

Thompson, G.A. and White, D.E. (1964) Regional Geology of the Steamboat Springs Area, Washoe County, Nevada. *USGS Professional Paper* 458-A, 52 p.

Vane, G., Green, R.O., Chrien, T.G., Enmark, H.T., Hansen, E.G., and Porter, W.M. (1993), The Airborne Visible/Infrared Imaging Spectrometer (AVIRIS). *Remote Sensing of Environment*, 44, p. 127–143.

Vaughan, R.G., Calvin, W.M., and Taranik, J.T. (2003). SEBASS Hyperspectral Thermal Infrared Data: Surface Emissivity Measurement and Mineral Mapping. *Remote Sensing of Environment*, 85, p. 48–63.

Vaughan, R.G. (2004). Surface Mineral Mapping at Virginia City and Steamboat Springs, Nevada with Multi-Wavelength Infrared Remote Sensing Image Data. *unpublished PhD Dissertation*, University of Nevada Reno, 259 p.

Vikre, P.G., McKee, E.H., and Silberman, M.L. (1988). Chronology of Miocene Hydrothermal and Igneous Events in the Western Virginia Range, Washoe, Storey, and Lyon Counties, Nevada. *Economic Geology*, 83, p. 864–874.

Vikre, P.G. (1998). Quartz-Alunite Alteration in the Western Part of the Virginia Range, Washoe and Storey Counties, Nevada. *Economic Geology*, 93, p. 338–346.

Vikre, P.G., Garside, L.J., Castor, S.B., Henry, C.D., Hudson, D.M., and McIntosh, W.C. (2003). Multiple Episodes of Magmatism, Quartz-Alunite Alteration, and Adularia-Sericite Precious Metal Mineralization, Western Virginia Range, Nevada. *Abstracts with Programs*, Geological Society of America, 35 (6), p. 401.

Watts, L.A., Davis, R.O., Granneman, R.D., LaVeigne, J.D., Chandos, R.A., Russell, E.E., and Cairns, B. (2001). Unique VISNIR-SWIR Hyperspectral and Polarimeter Measurements. In: *Proceedings of the 5th Airborne Remote Sensing Conference*, San Francisco, CA.

Whitebread, D.H. (1976). Alteration and Geochemistry of Tertiary Volcanic Rocks in Parts of the Virginia City, Quadrangle, Nevada. *USGS Professional Paper*, 936, 43 p.

Young, S.J., Johnson, B.R., and Hackwell, J.A. (2002), An In-scene Method for Atmospheric Compensation of Thermal Hyperspectral Data. *Journal of Geophysical Research*, 107 (D24), doi:10.1029/2001JD001266.